NUMERICAL INVESTIGATION OF PERFORMANCE OF KAPLAN TURBINE WITH DRAFT TUBE

Mohamed Adel and Nabil H. Mostafa

Mechanical Power Engineering Department, Engineering Faculty
Zagazig University, Zagazig, 44519, Egypt.
CORRESPONDING AUTHOR E-MAIL: M.ADEL@ZU.EDU.EG

ABSTRACT

This article presents a numerical investigation of the two phase flow in Kaplan turbine equipped with draft tube. The studied Kaplan turbine has a rotor with four blades mounted on a conical hub. The blade angle of the rotor is adjustable from 60° to 80°. A computational fluid dynamic code was used (CFDRC, 2008) to model the unsteady two-phase flow field around the blades of the Kaplan turbine at different angles and through the draft tube. The numerical simulation used the standard K-ε turbulence model to account for the turbulence effect. Pressure distribution and vapor volume fraction were computed at different blade angles. The results show that the cavitation phenomenon appeared at blade angle 80° and there is no cavitation appeared at blade angle 60° and 70°. Also there is no cavitation appeared through the draft tube and the installation of a draft tube downstream of the Kaplan turbine results the rejected kinetic energy reduced by 31.63%.

KEYWORDS : Two phase flow, Kaplan turbine, CFD, Draft tube and Simulation.

NOMENCLATURE

C_e, C_c	Phase change rate coefficients	
f	Vapor mass fraction	
k	Turbulence kinetic energy	m^2/s^2
N	Turbine rotational speed	r.p.m.
P	Fluid static pressure	N/m^2
p_{sat}	Saturation pressure	N/m^2
P'_{turb}	The magnitude of pressure fluctuations	N/m^2
P_t	Total pressure	N/m^2
P_v	Vapor pressure	N/m^2
R	Universal gas constant	Nm/mol.k
R	Phase change rate	
R_{en}	Reynolds number	
T	Fluid temperature	K
Δt	Physical time step	second
W	Molecular weight	kg/kg-mol

GREEK LETTERS

β_1	Blade inlet angle (angle between the tangent to camber line at inlet and the axial direction)	degree
β_2	Blade outlet angle (angle between the tangent to camber line at outlet and the axial direction)	degree
α_v	Vapor volume fraction	
α_g	gas volume fraction	
σ	Cavitation number $((p_\infty - p_v)/ (1/2\rho_l u^2))$	--

ρ	The mixture density	Kg/m^3
Γ	Effective exchange coefficient	

SUFFIXES

c	Bubble reduction and collapse
e	Bubble generation and expansion
Gas, G	Gaseous phase
L	Liquid phase
V	Vapor phases

1 INTRODUCTION

One of the most problems occurs in the hydraulic turbines is the cavitation phenomenon. The cavitation may cause noise pollution, erosion on the blade surface and the wall of the turbine, and a decrease of the water turbine efficiency Escaler, [4]. Cavitation occurs in the flow of water owing to regions of high flow velocity and the local static pressure decreases below the vapor pressure. Calculation of incipient cavitation is simple as one has just to find the lowest pressure indicating the cavitation inception once this lowest pressure reaches the vapor pressure. According to Sudsuansee et al, [15], cavitation may occur on the blade suction surface in region of low pressure or at the runner leading edge at off-design operation. A number of researchers have been investigating cavitation numerically. Balint et al, [1] carried out a numerical investigation by computing the 3D turbulent single phase flow in the Kaplan turbine runner. It was concluded that unsteady effects of the flow have been made mainly by the unsteady detachments of the cavitation at the blade suction side close to the trailing edge. Liu et al, [10] carried out a study of cavitating flow in a Kaplan turbine having numerical simulation with a cavitation model and a mixture two-phase flow model. The results show that the cavitation appears on the suction surface (S.S.); while in the other parts (runner flow passages, spiral casing, guide vanes, draft tube), there is not any cavity observed. Sedlář et al., [13] made Analysis of Cavitation Phenomena in Water and its Application to Prediction of Cavitation Erosion in Hydraulic Machinery. This article also shortly described the experimental research of the cavitating flow aimed at the validation of the erosion potential model, development of the nuclei-content measurement and the validation of the bubble nucleation model.Singh and Nestmann, [14] presented an experimental optimization of a free vortex propeller runner for micro hydro application. This paper presented a wide range of geometrical optimization steps carried out on a propeller runner, whose blades have been designed using the free vortex theory, and operating with a gross head from 1.5 to 2 m and discharge of approximately 75 l/s. Huang et al., [8] presented a numerical simulation of cavitation around a 2D hydrofoil. At a fixed attack angle, pressure distributions and volume fractions of vapor at different cavitation numbers were simulated, and the results on foil sections agreed well with experimental data. In addition, at the various cavitation numbers, the vapor fractions at different attack angles were also predicted. The vapor region moved towards the front of the airfoil and the length of the cavity grew with increased attack angle. The results show that this method of applying FLUENT to simulate cavitation is reliable. Kumara et al. [9] illustrated the benefits of cavitation monitoring in hydraulic turbines using vibration techniques. Mostafa and Adel [11] made a numerical simulation of cavitation and void growth inside the passage of the axial flow turbine. It was concluded that the cavity formation had mainly three stages. A numerical simulation of the flow in the draft tube of the Kaplan turbine was made by Tanase et al., [16].

The main objective of this article is to investigate numerically the two phase flow in Kaplan turbine equipped with draft tube, and study the effect of blade angle variations on the cavitation phenomenon in Kaplan turbine with specific interest in cavity geometry, pressure and void fraction fields. Besides, the effects of turbulence and fluid viscosity are included. The cavity shape over the blades and the 3-D flow field around the cavitating propeller will be determined. Finally the flow inside the draft tube passage will be simulated

2 THORETICAL BACKGROUND

The basic approach is to use standard viscous flow (Navier-Stokes) equations with provisions for variable density and a conventional turbulence model, such as K-ε model. A numerical model previously developed by CFDRC to solve (Navier- Stokes) equations Hinze, [7].

The mixture density (ρ) is a function of vapor mass fraction (*f*), which is computed by solving a transport equation simultaneously with the mass and momentum conservation equations. The ρ -*f* relationship is:

$$\frac{1}{\rho} \equiv \frac{f}{\rho_v} + \frac{1-f}{\rho_l} \quad (1)$$

In two-phase flows, the use of vapor volume fraction (α) is also quite common. Therefore, it is deduced from *f* as follows:

$$\alpha = f\frac{\rho}{\rho_v} \quad (2)$$

The transport equation for vapor is written as follows:

$$\frac{\partial}{\partial t}(\rho f) + \nabla\bullet(\rho \vec{V} f) = \nabla\bullet(\Gamma \nabla f) + R_e - R_c \quad (3)$$

The expressions of R_e and R_c have been derived from the reduced form of the Rayleigh-Plesset equation (Hammitt, [6]), which describes the dynamics of single bubble in an infinite liquid domain. The expressions for R_e and R_c are:

$$R_e = C_e \frac{V_{ch}}{\sigma}\rho_l\rho_v\sqrt{\frac{2}{3}\frac{p_{sat}-p}{\rho_l}}(1-f) \quad (4)$$

$$R_c = C_c \frac{V_{ch}}{\sigma}\rho_l\rho_v\sqrt{\frac{2}{3}\frac{p-p_{sat}}{\rho_l}}f \quad (5)$$

Cavitation normally takes place in the vicinity of low pressure (or locally high velocity) regions, where turbulence effects are quite significant. In particular, turbulent pressure fluctuations have significant effect on cavitating flows. The magnitude of pressure fluctuations is estimated by using the following empirical correlation (Pereira, et al., [12]):

$$P'_{turb} = 0.39\,\rho k \quad (6)$$

The vapor pressure threshold pressure value is as:

$$p_v = p_{sat} + 0.5p'_{turb} \quad (7)$$

It is well known that cavitating flows are sensitive to the presence of non-condensable gases. In most liquids, there is a small amount of non-condensable gases present in dissolved and/or mixed state. For example, laboratory water generally has 15 ppm air dissolved in it. In other applications, e.g., marine propellers, etc., this amount may be considerably larger. In this model, the non-condensable gas is included by prescribing an estimated mass fraction at inlet. This value is held constant throughout the calculation domain. However, the corresponding density (and hence volume fraction) varies significantly with local pressure. The perfect gas law is used to account for the expansion (or compressibility) of gas; i.e.

$$\rho_{gas} = \frac{WP}{RT} \quad (8)$$

The calculation of mixture density (equation 1) is modified as:

$$\frac{1}{\rho}=\frac{f_v}{\rho_v}+\frac{f_g}{\rho_g}+\frac{1-f_v-f_g}{\rho_l} \quad (9)$$

We have the following expression for the volume fractions of vapor (α_v) and gas (α_g):

$$\alpha_v=f_v\frac{\rho}{\rho_v} \quad (10)$$

$$\alpha_g=f_g\frac{\rho}{\rho_g} \quad (11)$$

And,

$$\alpha_l=1-\alpha_v-\alpha_g \quad (12)$$

The combined volume fraction of vapor and gas (i.e., $\alpha_v + \alpha_g$) is referred to as the Void Fraction (α). In practical applications, for qualitative assessment of the extent and location of cavitation, contour maps of void fraction (α) are important to determine bubbles location and shape.

3 COMPUTATIONAL ANALYSIS

The numerical simulation was done using a 3-D Navier-Stokes code (CFDRC, 2008) to model the two phase flow field around a 3D rotor in a cavitating Kaplan turbine. This code employs a homogenous flow approach, also known as Equal-Velocity-Equal-Temperature (EVET) approach (CFDRC, [2] and [3]) and Fukaya, et al., [5].

The governing equations are discretized on a structured grid using an upwind difference scheme. The numerical simulation used the standard K-ε turbulence model to account for the turbulence effect. The cavity shape was determined. Also, various variables were calculated, such as void fraction, mass fraction, pressure and velocity contours.

It is clear that the full cavitaion model used in this simulation includes a lot of effects which were previously ignored in the previous studies, such as unsteady, fluid viscosity and turbulence.

4 BOUNDARY CONDITIONS

In this case of a four-blade Kaplan turbine, twenty blocks were used to generate the 3D rotor model as shown in Fig. 3. The structured grid is consisted of about 220,400 nodes. The propeller diameter is 4 in. (101 mm). Reynolds number is about 333,000. The structured grid geometry of the rotor is constructed at three blade angles 60^o, 70^o and 80^o as shown in Fig. 4. The unsteady time step was $1.2x10^{-4}$ sec. The computational time was about 20 minutes for one time step. The computer used was Intel Core i5 Processor 2.4 GHz, and 4 GB RAM.

5 RESULTS VALIDATION

Fig. 5 shows a comparison between the present numerical result, which is presented in Fig. 5a, and the result of **Balint et al. [1]**, Fig. 5b, shows an acceptable agreement. Pressure distribution and void fraction distribution around the hydrofoil are validated by comparing the predicted numerical results with the experimental results of **Sedlář et al. [13]** as shown in Fig. 6 and Fig. 7.

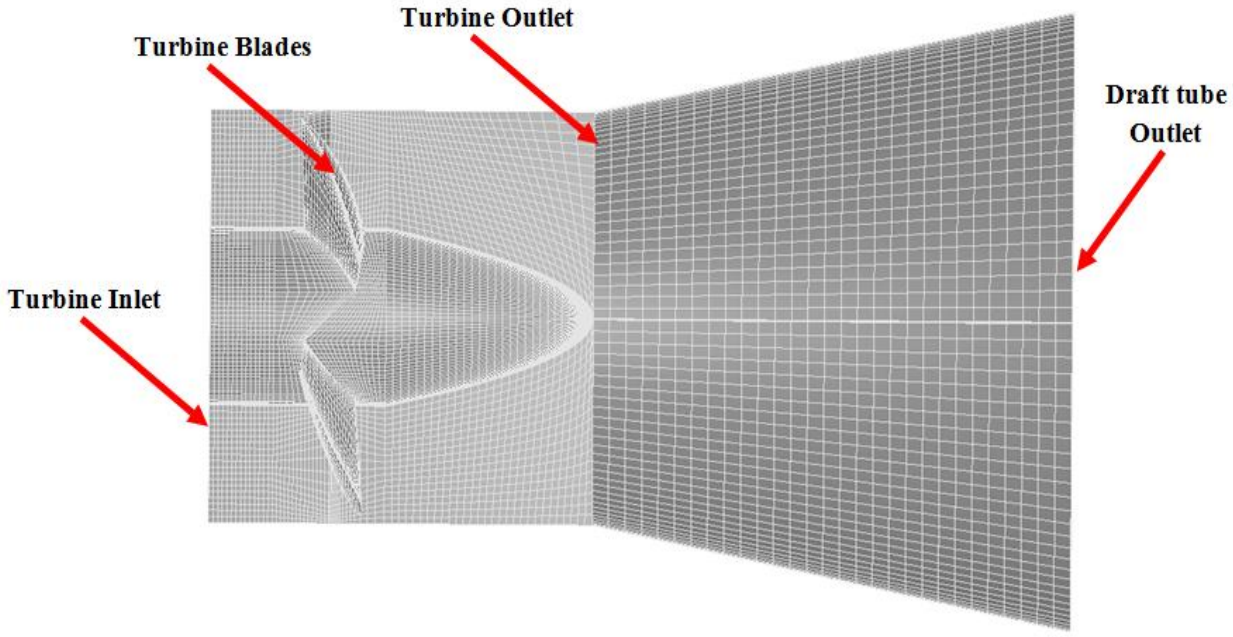

Figure 3. Geometry technique for the Kaplan turbine equipped with draft tube.

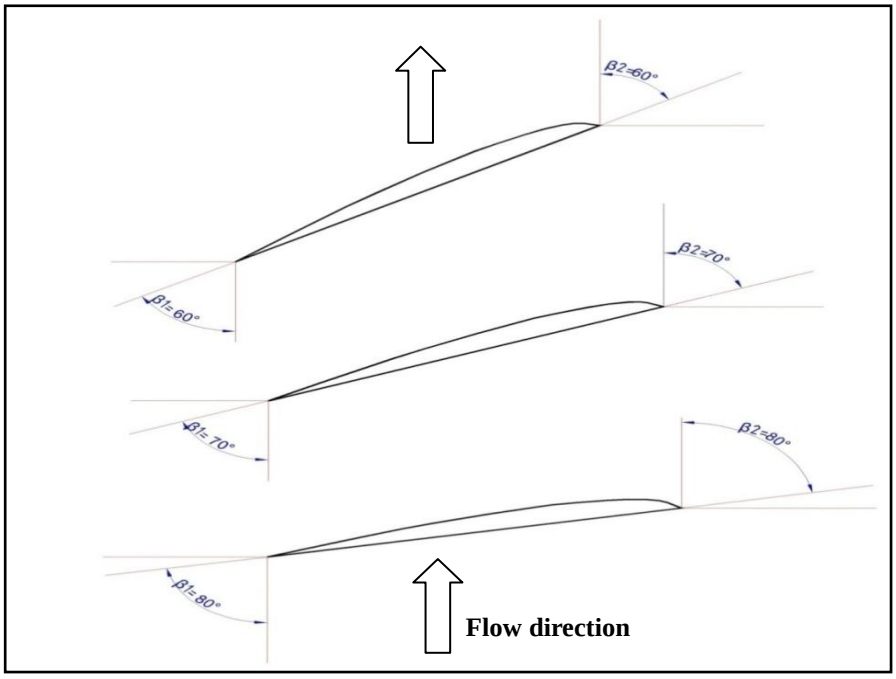

Figure 4. Blade inlet and outlet angles

6 RESULTS AND DISCUSSION

The contours of computed vapor volume fraction on the hydrofoil at blade angles 80°, 70°, and 60° are presented in Figs. 8a, b, c respectively. It is obvious that cavitation does not appear at blade angles 60° and 70° while it is appeared at blade angle 80° at the leading edge of the suction side due to the decrease in static pressure below the vapor pressure. The computed density contours on the hydrofoil at blade angles 80°, 70°, and 60° are presented in Figs. 9a, b, c respectively. It is obvious that is no change in density at blade angles 60° and 70°, while the density

decreases sharply at blade angles 80° at the leading edge of the blades due to the decrease in static pressure below the vapor pressure and the increasing in the blade inlet angle.

Also the flow through draft tube was simulated at the conditions of cavitation (Q=20 L/s, 2000 rpm, β_1=80° and β_2=80°). Fig. 10a shows the static pressure computational contours through draft tube. The static pressure still above the vapor pressure of the water and didn't decreased under the vapor pressure through the whole area of the draft tube. And it is obvious that the static pressure increased from the inlet to the outlet of the draft tube this is due to the decreasing in the rejected kinetic energy. Fig. 10b displays the vapor volume fraction computational contours through draft tube. It is obvious that there is no cavitation appeared through the whole area of the draft tube. Fig. 11a shows the velocity computational contours through draft tube. It is obvious that the inlet velocity to draft tube was decreased from 2.8 m/s to 1.6 m/s at the draft tube exit. This means that the rejected kinetic energy was reduced by 31.63%. Fig. 11b shows the static pressure variations versus the draft tube length. The static pressure is increased from the inlet to the outlet of draft tube this is due to the decreasing in the velocity magnitude.

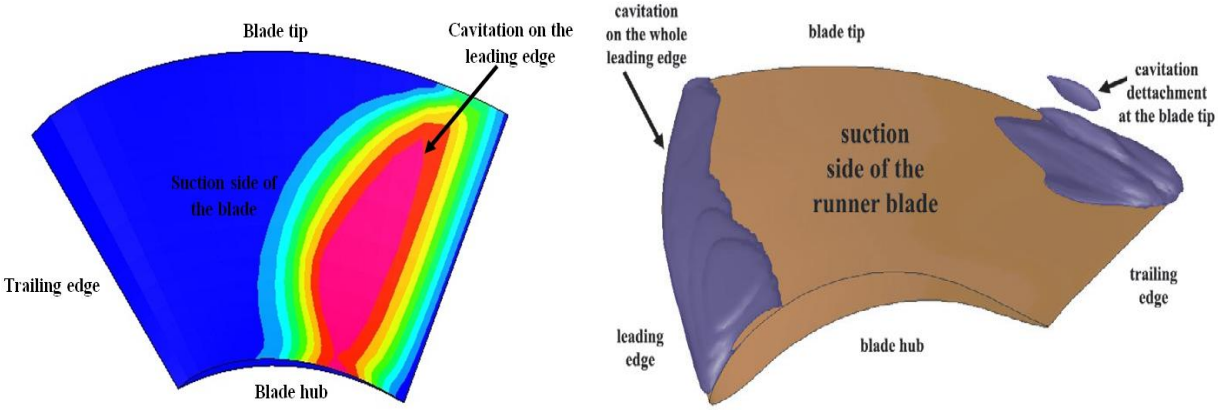

a) Cavitation distribution on the runner blade. **[Present study]**

b) Cavitation distribution on the runner blade. **[Balint et al, 2004]**

Figure 5. Comparison between the cavitation distribution on the blade with Balint et al. results.

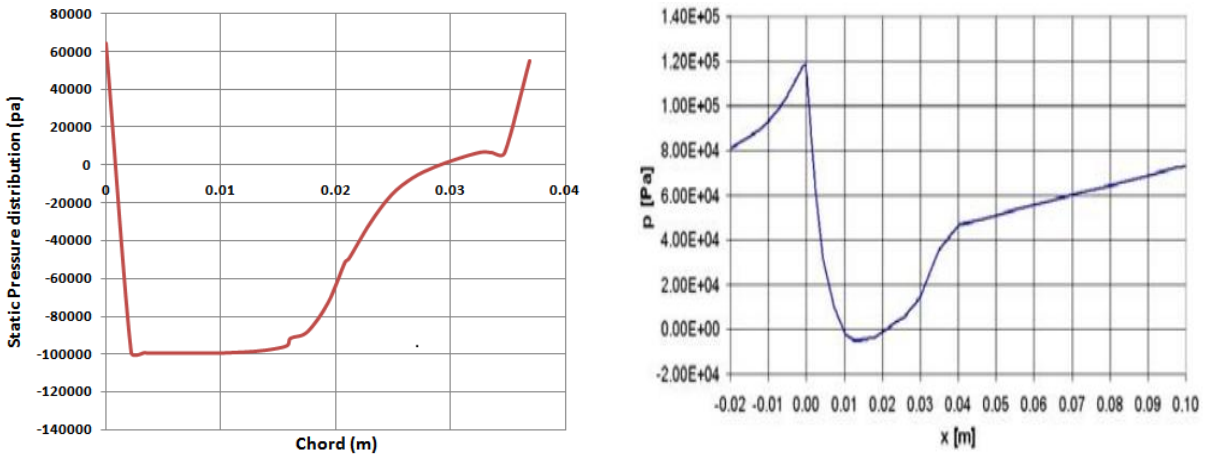

a) Pressure distribution on the hydrofoil after 0.075 Sec. **[present study]**

b) Pressure distribution on the hydrofoil **[Sedlář et al., 2008].**

Figure 6. Comparison between the pressure distribution on the hydrofoil with Sedlář et al. results.

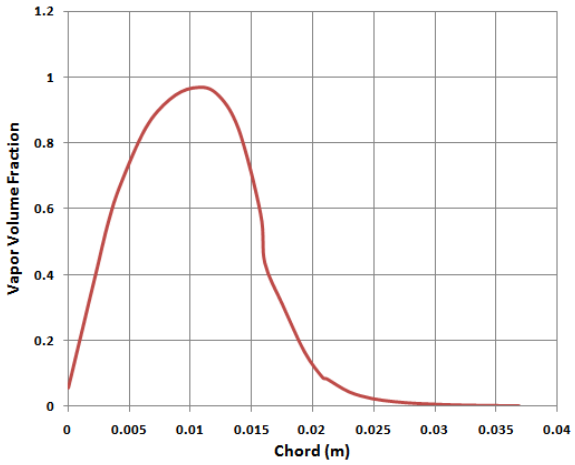

a) Void fraction distribution on the hydrofoil after 0.075 Sec. **[Present study].**

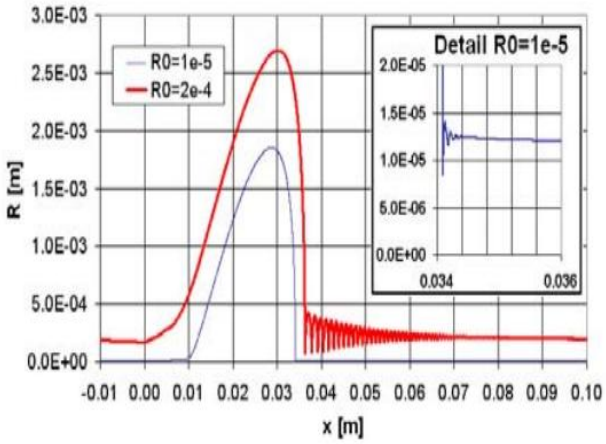

b) cavitation nucleus on the hydrofoil **[Sedlář et al., 2008].**

Figure 7. Comparison between void fraction distribution on the hydrofoil with Sedlář et al. results.

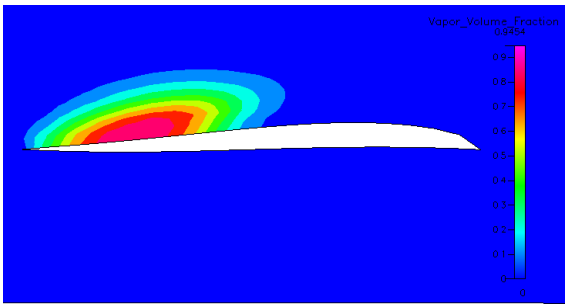

Figure 8. a Vapor volume distribution on the hydrofoil at 2000 rpm, $\beta_1 = 80^o$and $\beta_2 = 80^o$.

Figure 9. a Density distribution on the hydrofoil at 2000 rpm, $\beta_1 = 80^o$and $\beta_2 = 80^o$.

Figure 8. b Vapor volume distribution on the hydrofoil at 2000 rpm, $\beta_1 = 70^o$and $\beta_2 = 70^o$.

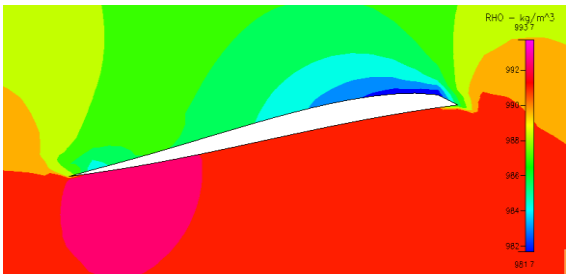

Figure 9.b Density distribution on the hydrofoil at 2000 rpm, $\beta_1 = 70^o$and $\beta_2 = 70^o$.

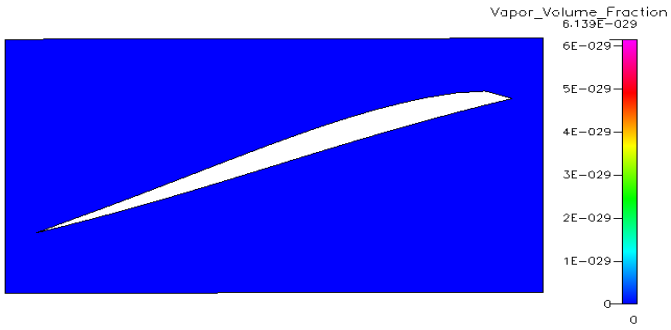

Figure 8.c Vapor volume distribution on the hydrofoil at 2000 rpm, $\beta_1 = 60^o$and $\beta_2 = 60^o$.

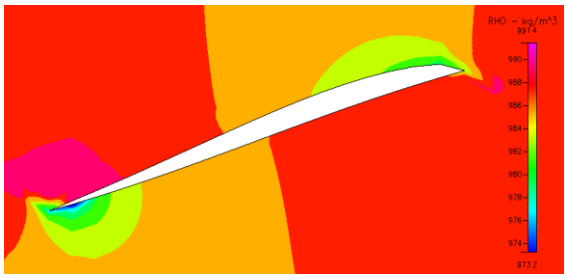

Figure 9.c Density distribution on the hydrofoil at 2000 rpm, $\beta_1 = 60^o$and $\beta_2 = 60^o$.

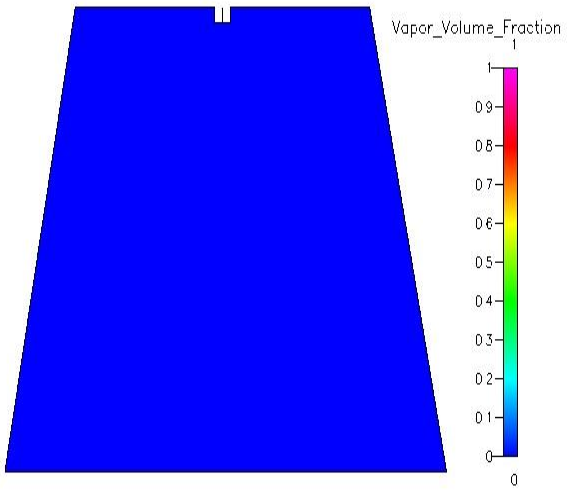

Figure 10.a Vapor volume distribution through draft tube.

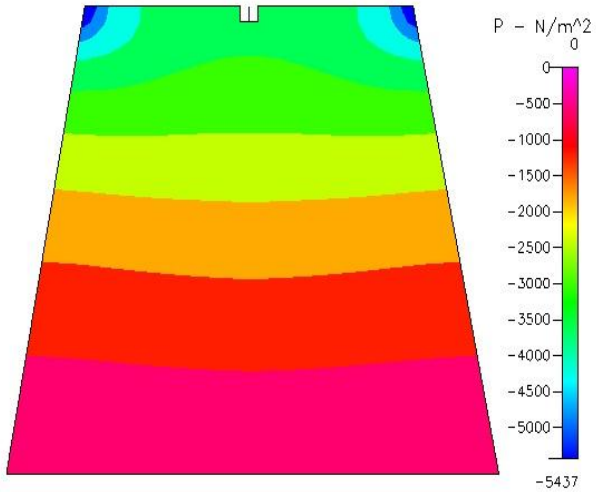

Figure 10. b Static Pressure distribution through draft tube.

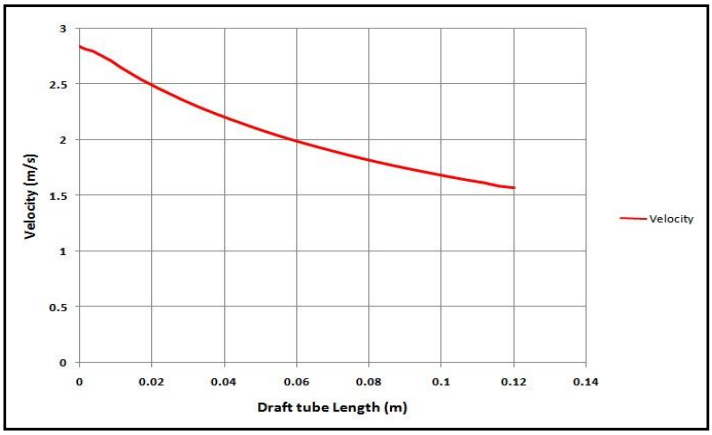

Figure. 11. a Velocity magnitude variations versus draft tube length.

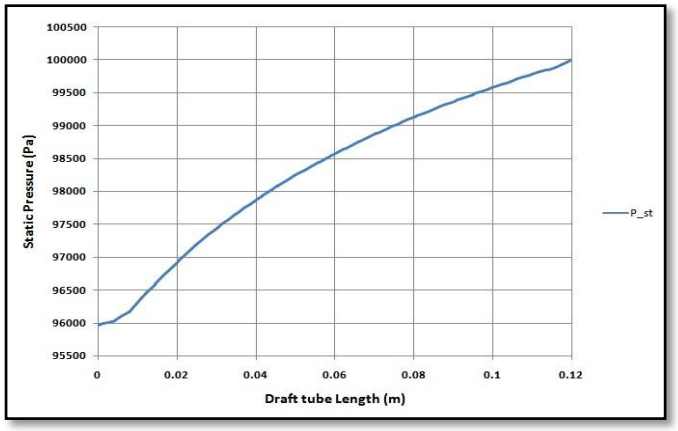

Figure 11. b Static pressure variations versus draft tube length.

7 SUMMARY AND CONCLUSIONS

A numerical investigation of the performance of Kaplan turbine was performed using a commercial CFD code called CFD-RC which uses the "The full cavitaion model" to predict the cavitaion in axial turbine.

From the results of the present study, the conclusions are as follows:

1- Cavitation occurred at blade angle 80^o and not appeared at blade angles 60^o and 70^o.
2- By adjusting the blade angle to 60^o or 70^o, cavitation can be avoided.
3- The highest performance of Kaplan turbine could be obtained at blade angles 60^o or 70^o because there is no cavitation observed over the blades.
4- There is no cavitation appeared through the draft tube.
5- The installation of a draft tube downstream of the Kaplan turbine reduces the rejected kinetic energy by 31.63%.

REFERENCES:

Balint, D., Resiga, R., Muntean, S., Ruprecht, A., and Goede, E., High performance computing of self induced unsteadiness cavitating flows in hydro turbine. Romania: University Politehnica of Timisoara, National Center for Engineering of Systems with Complex Fluids, 2004.

CFD-ACE V2008 Modules Manual – Volume 1, May 1, 2008.

CFD-ACE V2008 User Manual – Volume 1, May 1, 2008.

Escaler, X., Egusquiza, E., Farahat, M., Avellan, F., and Coussirat, M., Detection of cavitation in hydraulic turbines. Mechanical Systems and Signal Processing, 2006. 20, pp 983-1007.

Fukaya, M., Okamura, T., Tamura, Y., Matsumoto, Y., Prediction of Cavitation Performance of Axial Flow Pump by Using Numerical Cavitating Flow Simulation with Bubble Flow Model. *Fifth International Symposium on Cavitation* ,Osaka, Japan. November 1-4, 2003.

Hammitt, F. G., Cavitation and multiphase flow phenomena. McGraw-Hill International Book Co., New York. , 1980.

Hinze, J.O., Turbulence. McGraw-Hill Book Co., Second Edition, 1975.

Huang, S., He, M., Wang, C., and Chang, X., Simulation of Cavitating Flow around a 2-D Hydrofoil. J. Marine. Sci. Appl. Vol. 9: pp63-68, 2010.

Kummar, P., and Saini, R., P., "Study of cavitation in hydro turbines" *j. of renewable and sustainable energy,* Vol. 14, issue 1, pp 374-383, 2010.

Liu, S., Chen, Q., and Wu, Y.," Unsteady Cavitating Turbulent Flow Simulation In A Kaplan Turbine", Proceedings of the 2nd IAHR International Meeting of the Workgroup on Cavitation and Dynamic Problems in Hydraulic Machinery and Systems, 2007.

Mostafa, H. N. and Adel, M., "Unsteady Numerical Simulation of Cavitation in Axial Turbine" Journal of CFD letters, Vol. 4, Sept., 140-149, 2012.

Pereira, F., Salvatrore, F. and Felice F., Measurement and Modeling of propeller cavitation in uniform inflow. Transactions of the ASME, Journal of Fluid Engineering, 126, pp. 671-679, 2004.

Sedlář, M., Zima, P., Ně mec, T., and Maršík, F., Analysis of Cavitation Phenomena in Water and its Application to Prediction of Cavitation Erosion in Hydraulic Machinery. *ICPWS XV*, Berlin, 2008.

Singh, P., and Nestmann, F., Experimental optimization of a free vortex propeller runner for micro hydro application. Experimental Thermal and Fluid Science 33, pp 991–1002, 2009.

Sudsuansee, T., Nontakaew, U., and Tiaple, Y., "Simulation of leading edge cavitation on bulb turbine*", Songklanakarin J. Sci. Technol.,* Vol. 31, pp. 51-60, 2011.

Tanase, N., O., Bunea, F. and Ciocan, G., D., "Numerical Simulation Of The Flow In The Draft Tube Of The Kaplan Turbine" U.P.B. Sci. Bull., Series D, Vol. 74, Iss. 1, 2012.